Accessing the fractal dimension of free clusters in supersonic beams

2011 New J. Phys. 13 023009

(http://iopscience.iop.org/1367-2630/13/2/023009)

New Journal of Physics
The open-access journal for physics

Accessing the fractal dimension of free clusters in supersonic beams

T Mazza[1], M Devetta[1], P Milani[1], G Bongiorno[1,3], M Coreno[2] and P Piseri[1,4]

[1] Dipartimento di Fisica and CIMAINA, Università degli Studi di Milano, Via Celoria 16, I-20133 Milano, Italy
[2] CNR-IMIP, Area della Ricerca di Roma I, Via Salaria Km 29.3, I-00016 Roma, Italy
E-mail: paolo.piseri@fisica.unimi.it

New Journal of Physics **13** (2011) 023009 (12pp)
Received 3 November 2010
Published 2 February 2011
Online at http://www.njp.org/
doi:10.1088/1367-2630/13/2/023009

Abstract. In this paper a method for the quantitative determination of a morphology descriptor of free clusters with complex nanostructure is presented and applied to transition metal nanoparticles produced by a pulsed vaporization source. The method, which is based on the low-pressure aerodynamic mobility of neutral particles, can be applied as a characterization tool to a broad class of gas-phase nanoparticle sources for on-line investigation of particle growth and for quantifying coalescence versus agglomerate aggregation. We report on the application of this method for the characterization of free titanium clusters produced by a pulsed microplasma cluster source in the size range of approximately 300–6000 atoms. The clusters have an open fractal-like structure, with the fractal dimension depending on their thermal history during growth and evolving towards softer aggregates for longer residence times where lower-temperature conditions characterize the growth environment.

[3] Present address: Fondazione Filarete, Viale Ortles 22/4, I-20139 Milano, Italy.
[4] Author to whom any correspondence should be addressed.

Contents

1. Introduction

The study of isolated nanoparticles produced in the gas phase is of fundamental importance for understanding how properties of matter evolve from atomic and molecular features to those typical of bulk materials. Besides the fundamental interest, the bottom-up approach, which is based on the assembling of novel materials with tailored properties from nanoscale building blocks, relies on the possibility of establishing clear relationships between the assembled materials and nanoscale building blocks. To account for the electronic properties of free metallic nanoparticles, they are often modelled as spherical objects [1] although the characterization of nanostructured solids obtained from the assembling of nanoparticles produced in the gas phase suggests that this is a crude oversimplification neglecting the structural complexity of nanosized objects and its influence on the cluster-assembled system [2]. A multi-parametric approach involving, besides size, the morphology, stoichiometry and spatial distribution of nanoparticles is thus needed, especially in view of large-scale applications based on the assembling of nanoparticles produced in the gas phase. This is particularly important for an adequate description of systems prepared aiming at applications and grown with large-scale production technologies such as inert-gas-condensation (IGC) sources [3] where nanoparticles undergo different and complex stages of growth such as inception, coalescence and agglomeration [4]: nanoscale morphology is indeed strongly affected by particle growth conditions and cluster–cluster coagulation can lead to the formation of ramified or fractal-like nano-objects with peculiar properties arising from either the individual constituents or the collective properties of the aggregates [2]–[6].

Although a number of studies have been dedicated to the theory of IGC particle growth [2, 4, 5, 7, 8], only few *in situ* experimental investigations are reported in the literature on the formation process of fractal particles in nanoparticle sources; most of them have been performed on rather large systems using ion mobility methods or small angle x-ray scattering (SAXS) [9]. The problem of determining fractal dimension from dynamic properties measurements has been discussed in detail by Schmidt-Ott [10]. Unambiguous determination of the morphology of free isolated particles is a very difficult task, and most of the routes of choice such as differential mobility analysis (DMA) [11], light scattering [12] or mobility particle sizing combined with electrical low-pressure impaction (ELPI) [13] require complementary information, typically from accessory microscopy studies on deposited clusters. Microscopy characterization techniques can also be misleading, as deposited clusters suffer from a number of processes upon landing such as structure distortion or fragmentation [14] or further aggregation and possibly coalescence; all these issues are even more critical when dealing with

non-compact objects, and full gas-phase methods such as aerosol photoemission [10] should be preferred. In recent years, a great deal of interest has been directed to the application of gas-phase ion mobility measurements to macromolecular and cluster systems as the route of choice for the separation of isomers with different geometries; the technique has proven to be effective for probing very small ions [15]. Evidence for a structural transition for a given cluster size has been reported by Jarrold and co-workers from ion mobility measurements on Si_n [16] and Ge_n [17] ions.

In this paper we present an experimental approach for a quantitative morphological characterization of free, isolated clusters seeded in a supersonic beam. Our approach is based on the same principle as that exploited in ion mobility measurements, with the advantage of providing access for neutral particles to a scale-independent effective parameter, namely the particles' fractal dimension, inferred from the analysis and modelling of the particle mass-to-velocity relationship in supersonic beams. As it extracts a scaling law from a representative ensemble of many particles, the method actually deals with the determination of the fractal dimension characterizing a sample consisting of a set of aggregates, and is not suitable for the determination of the corresponding property for a given fractal object alone. We report then a study on the morphology of titanium nanoparticles produced by a pulsed microplasma cluster source (PMCS) [18]; owing to its pulsed nature the source can produce clusters experiencing a wide range of different growth conditions [19], which makes the possibility of applying a structural characterization method particularly significant.

2. Model description

The properties of a supersonic beam are mainly determined by the size and shape of the nozzle and by the thermodynamic properties of the gas upstream of the nozzle [20]. An approach by means of simple models can provide appropriate semi-quantitative predictions [20]. Ideal thermodynamic analysis based on the first law can be employed to determine stream velocity, temperature, pressure and density along the jet axis versus distance from the nozzle. In particular, the maximum terminal velocity v_{gas} of the molecules (mass m_{gas}) is given by

$$v_{\mathrm{gas}} = \sqrt{2k_{\mathrm{B}}\gamma \cdot T_{\mathrm{s}}/\left(m_{\mathrm{gas}}\,(\gamma-1)\right)}, \tag{1}$$

where γ is the heat capacity ratio, T_{s} the stagnation temperature before the expansion and k_{B} the Boltzmann constant. The presence in the beam of heavy species—such as nanoparticles—generally introduces severe complications in the analysis; the problem can nevertheless be easily treated when the species are diluted in a carrier gas with very low relative concentration. In this case, the thermodynamic properties of the expansion can be assumed to be not affected by the presence of the seeding particles [21] that are accelerated up to a size-dependent terminal velocity by the collisions with the carrier gas [22]. This effect on cluster velocity of the finite number of collisions occurring before transition to the collision-less free molecular regime characteristic of molecular beams is usually called 'velocity slip' [23] and can be effectively modelled through a dynamic shape factor in the free molecular Epstein regime [24], i.e. taking into account the size dependence of cluster inertia and of the collisional cross section determining the collision rate with carrier gas molecules. An expression for this model was originally formulated by Wrenger and Meiwes-Broer [25] under limiting assumptions (central and elastic collisions between clusters considered as hard spheres); a more general statement

is derived in the appendix from the single postulate of momentum conservation, leading to the following expression:

$$v\,(m;\sigma) = v_{\mathrm{gas}} \cdot \left[1 - \left(\frac{m - m_{\mathrm{gas}}}{m + m_{\mathrm{gas}}}\right)^{\beta\cdot\sigma}\right]. \tag{2}$$

This expression puts in explicit form the fact that clusters seeded in a supersonic expansion are accelerated along the jet axis by collisions with the expanding gas molecules, the number of forward kicks being determined according to the particle collisional cross section and the effect of each one being related to the particle mass and an additional scaling parameter characteristic of the scattering process. An accurate measurement of the velocity-to-mass relation characterizing a set of clusters can therefore bring information on the morphology on the scale of carrier gas molecules collisional cross section of the probed ensemble; an explicit form for cluster morphology description enters into the model through the scaling law connecting σ to m.

According to a working definition of the fractal dimension characterizing a set of aggregates as the exponent describing the scaling of objects' size S against a characteristic linear dimension R ($S \propto R^D$), a relation can be obtained between the fractal dimension D for clusters' volume in three dimensions (3D) and fractal dimension D^* for the corresponding projected area in 2D. In the case of infinite self-similar objects this relation can be simply recognized in $D^* = \min(2, D)$ [26], while the case of real fractal-like objects has been discussed in detail by Nelson *et al* [27], who derived the expression relating D and D^* as a function of an observation scale parameter X (defined in reduced units relative to object linear dimension) that accounts for the finite resolution of the observation method or for the lower boundary to the scale of the fractal-like physical object imposed by finite primary particle size of the aggregates.

For a physical fractal-like object consisting of an aggregate formed by a number of homogeneous primary particles, we have $m \propto R^D$ and, being the geometrical cross section for the gas–particle collision proportional to the aggregate's projection area, $\sigma \propto R^{D*}$. We can thus write

$$\sigma \propto m^{D^*/D} = m^{\xi}, \tag{3}$$

where ξ is defined as D^*/D. A given $\xi \leqslant 1$ generally corresponds to two possible distinct solutions for the fractal dimension D, one in the range $2 \leqslant D \leqslant 3$ given by $D = 2/\xi$ and the other in the range $1 \leqslant D < 2$ that, if an estimate for the observation scale is available, can be determined using the expression given by Nelson *et al* [27]. In the process of probing cluster geometry through atomic collisions, the observation scale is of the order of the collision diameter of the carrier gas (~0.27 nm in the case of He [28]). The assignment of a fractal character to clusters and nanoparticles is also generally limited by an inner scale imposed by the size of the primary particles forming the aggregate (which can be larger than the atomic scale in the presence of hierarchical aggregation of compact primary particles into fractal-like super-aggregates). According to Nelson *et al* [27] this finite component size does not affect the apparent dimension D^* as long as it is considerably smaller than the aggregate size. As illustrated hereafter, the proposed method for the characterization of the σ to m scaling behaviour provides therefore access to a quantitative determination of the fractal dimension of the aggregates, restricting indecision to two distinct solutions that generally correspond to distinct physical situations, which are very far and which can therefore be sorted out on the basis of very limited previous knowledge of the system under study. The most peculiar aspect of this

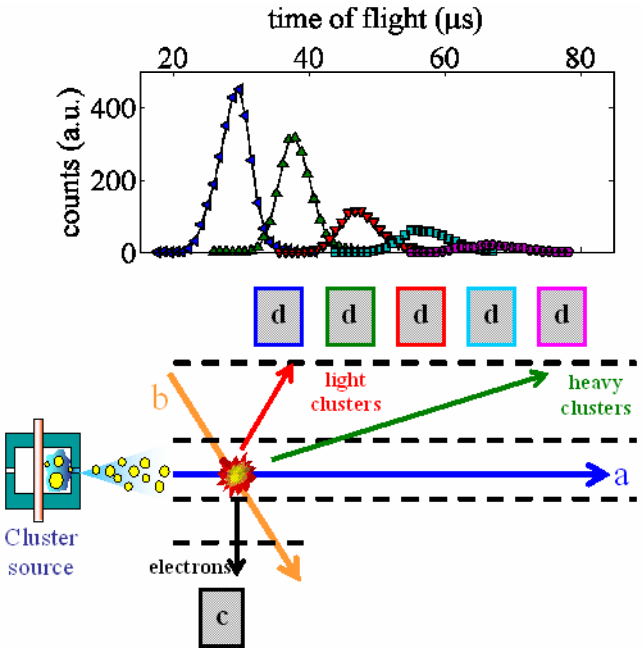

Figure 1. Top: TOF signal collected by channel electron multipliers (CEM) at different positions: CEM no. 1, blue leftward triangles; CEM no. 2, green upward triangles; CEM no. 3, red downward triangles; CEM no. 4, cyan squares; CEM no. 5, violet circles. Bottom: schematic representation of the apparatus for mass-to-velocity relationship measurement in a seeded supersonic beam. The seeded supersonic beam (a) crosses a photon beam (b) in the accelerating region of a linear TOF mass spectrometer equipped with a position-sensitive ion detector array (d). The transverse velocity of the clusters in the molecular beam makes the different detectors of the array sensitive to different windows in the TOF spectrum.

method is that it provides a fractal dimension parameter associated with a cluster population, and not with a single object. Sampling from a set of many particles of different sizes is individuated indeed as the most effective route for mapping the system under study at different length scales using a single probe with fixed scale—the colliding atoms.

3. Experimental procedure

Our experimental setup for the mass and velocity measurement of aerodynamically accelerated neutral particles is based on a time-of-flight (TOF) mass spectrometer installed with its axis perpendicular to the propagation direction of a seeded supersonic cluster beam, and equipped with a position-sensitive detector; a suitable ionization source producing limited or controlled fragmentation and uniform charge state is also needed (figure 1). Spatially resolved TOF mass spectrometry enables reconstruction of the velocity of the clusters, as the position of the detected ion relative to the ionization point, combined with the TOF, provides a well-defined velocity measurement and allows us to link this information with a mass spectrometric size determination.

Measurement of the cluster mass-to-velocity relationship has been carried out crossing the supersonic beam with a VUV-photon beam in the accelerating region of a linear TOF mass spectrometer equipped with a CEM array (figure 1). After VUV-induced ionization, photoemitted electrons and photoionized clusters are accelerated in opposite directions perpendicularly to the beam and are collected by the respective detectors. TOF of clusters is measured by photoelectron–photoion-coincidence (PEPICO) [19]. During their flight, clusters travel along the beam direction conserving the corresponding momentum component; this makes each detector of the CEM array sensitive to a given beam velocity-dependent window in the TOF mass spectrum. Although spatial resolution of the CEM array detector is very limited, a well-defined velocity measurement related to a specific mass value can be determined by analysing the mode of the portion of the TOF spectrum recorded by each single detector in the array, and using the detector centre for the position.

The supersonic cluster beam apparatus used for our study is based on a PMCS combined with an aerodynamic lens system; details of the configuration can be found in [19]. The working principle of the PMCS is described in detail elsewhere [18, 29]. Briefly, the injection in the source cavity of inert gas from a high-pressure reservoir is followed by a very short (a few tens of μs) and intense (a few hundreds of amperes) discharge. Due to aerodynamics, a localized high pressure region is formed at the target surface and ablation of the metallic target through ion bombardment is thus confined; subsequent condensation of sputtered atoms results in cluster nucleation. A gas–cluster mixture is then extracted from the PMCS expanding in a seeded supersonic free jet into a vacuum vessel and forming a particle beam. The sample/carrier gas ratio in the expansion is in the range of 10^{-4} (atomic ratio) so that the high dilution condition is satisfied, and the gas terminal velocity from the expansion can be conveniently described by equation (1) with $\gamma = 5/3$. According to nozzle conductance, the clusters spend some time in the source before being drawn into the expanding jet. With an aerodynamic lens nozzle, the typical residence time can last up to tens of milliseconds and a broad distribution of different particle thermal histories is observed. The analysis of the velocity-to-mass relationship can be performed keeping track of the timing within cluster beam pulses—i.e. resolving different residence times for the clusters—by the acquisition of electron and ion detection times relative to a trigger signal syncing acquisition with the cluster source repetition cycle [19].

Measurements have been carried out on free titanium nanoparticles tuning the monochromator of the *GasPhase* beamline at the *Elettra* Synchrotron Radiation facility [30] in the 450–470 eV photon energy region (around the Ti2p edge), in order to maximize the yield of coincidence events from the clusters and to minimize the contributions to the electron and ion signals from the ionization of background gas present in the vacuum vessel (base pressure during the experiment was $<5 \times 10^{-9}$ mbar). Interaction with VUV photons induces photofragmentation of clusters and the formation of different multiply charged states after core-level photoionization [31, 32]. The occurrence of these processes complicates significantly the interpretation of TOF spectra and thus introduces some limit to the possibility of establishing a mass-to-velocity relationship. Anyway, the experimental apparatus presented in [19] gives access to single event reconstruction analysis, allowing (i) unambiguous discrimination of correlated and independent ion detection events that makes it possible to single out, after taking into account also ion detection efficiency limits, the contribution from unfragmented clusters to the TOF spectra; (ii) the evaluation of the overall fraction of reconstructed events, from which, after a reliable estimate for electron detection efficiency, a mean charge state value can

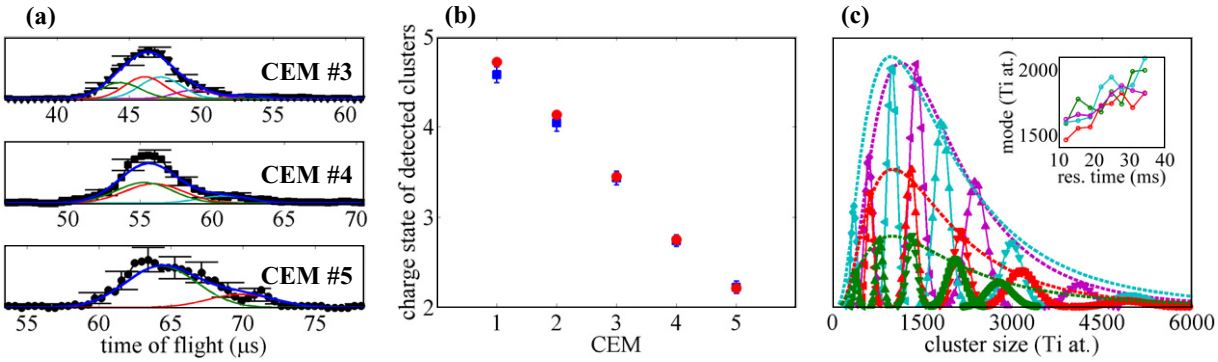

Figure 2. (a) Ti clusters' TOF distributions recorded by elements no. 3 (top), no. 4 (centre) and no. 5 (bottom) of the CEM array, for clusters with residence time in the 17–20 ms interval. For each spectrum, the fitting by superposing Gaussian-shaped modes corresponding to different charge states is shown (charge states: green = 2, red = 3, cyan = 4, magenta = 5 and bold blue = sum of all modes). (b) The average charge value (red circles) of clusters detected by each CEM element from the weighted mean of the charge-dependent modes is compared with the clusters population charge state (blue squares) determined from the evaluation of the overall fraction of reconstructed events [31]. (c) The contributions to the TOF spectra recorded in the 23–26 ms residence time window by the different CEM elements (symbols as in figure 1) from twofold, threefold, fourfold and fivefold charged clusters (colours as in figure 2(a)) are plotted here versus the cluster size abscissa. The log-normal mass distribution as obtained by fitting the values at peak maxima for each of these charge state contributions is also plotted (broken lines). The inset shows the residence time dependence for the best-fit log-normal mode.

be obtained [31] and compared with the charge state measurement as obtained from the TOF spectra fitting procedure described hereafter.

4. Results and discussion

TOF spectra from clusters selected in a given residence time window and collected by three different elements of the CEM array are shown in figure 2(a); TOF spectra from other residence time windows and other CEM array elements (not shown) show analogous features. Spectra are modelled as the sum of contributions from differently charged clusters that, after ionization, share similar mass-to-charge ratios and velocities. The TOF spectrum collected by each element of the CEM array has been analyzed by a fitting procedure resolving charge-dependent modes. Modes are described by Gaussian lineshapes accounting for cluster velocity distribution and, through their amplitude, for the ion detection efficiency characterizing the detector. The fitting procedure identifies modes' position and intensity with the following conditions: (i) the average charge state of the measured clusters population must match the value obtained from detector efficiency considerations; this puts a constraint on the relative weight of the different charge state contributions for each CEM (figure 2(b)); (ii) for each charge state the intensities of the contributions to the mass spectrum collected by the different CEMs must overlap with a single

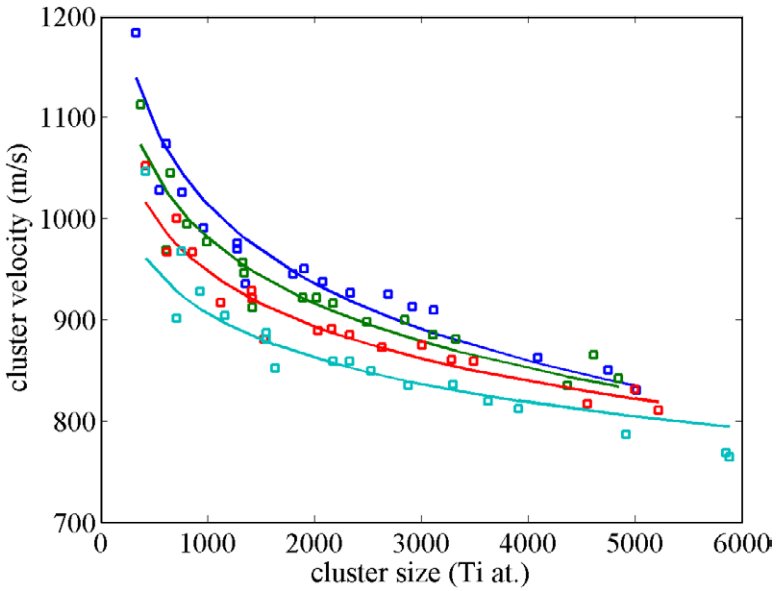

Figure 3. The mass-to-velocity relationship for titanium clusters from selected residence time windows (centred around 18 ms (blue), 25 ms (green), 31 ms (red) and 37 ms (cyan)). Each point is obtained by central values (TOF and detector position) from a single mode with a defined charge state (and thus unambiguously determined mass from TOF). Full lines represent the best fit to the experimental data with the model described in the text.

log-normal curve describing the cluster mass distribution (figure 2(c)); both the mode and the geometric standard deviation parameters are determined by the fitting procedure and the average mass of clusters increases with increasing residence time (inset of figure 2(c)).

Within the present description each mode position identifies a data point in the mass–velocity diagram (figure 3); the analysis of the TOF spectra from different CEMs in the array and for different residence time values (t_{res}) provides a measurement of the velocity-to-mass relationship $v = v(m,\ t_{\mathrm{res}})$ over a wide mass range (∼300–6000 Ti atoms) and over a large residence time span (sufficient statistics to perform the described fitting procedure is available in the 15–40 ms interval).

A least-square fitting of the $v = v(m,t_{\mathrm{res}})$ data points with the model expressed in equation (2), where the scaling law connecting σ to m is put in explicit form by $\beta \cdot \sigma = \tilde{\beta} \cdot m^{D^*/D} = \tilde{\beta} \cdot m^{\xi}$, allows the mapping of the fractal dimension parameter describing the morphology of the particles populating different portions of the pulsed cluster beam.

A set of links between the fitting parameters is assumed in order to reduce the number of degrees of freedom and use the acquired data statistics in the most effective way. A quadratic dependence of $\xi = D^*/D$ on the residence time $\xi = \xi_0 + \xi_1 \cdot t_{\mathrm{res}} + \xi_2 \cdot t_{\mathrm{res}}^2$ is assumed as a second-order approximation in order to allow the appearance of any existing trend in cluster fractal dimension.

Carrier gas velocity and the effective collision number pre-factor $\tilde{\beta}$ entering the expression are described, in their dependence on the residence time t_{res}, by [22]

$$v_{\mathrm{gas}} = v_{\mathrm{gas},0} \cdot \mathrm{e}^{-t_{\mathrm{res}}/2\tau}, \tag{4}$$

$$\tilde{\beta} \propto r \cdot \Delta t \propto \left(n_{\mathrm{gas}} \cdot v_{\mathrm{gas}}\right) \cdot v_{\mathrm{gas}}^{-1} = n_{\mathrm{gas}}, \tag{5}$$

where r is the density of atomic current characterizing the expansion, which is proportional to gas density n_{gas} multiplied by gas velocity v_{gas} [33]; under adiabatic conditions the gas density scales as $T_{\mathrm{s}}^{1/(\gamma-1)}$, i.e. $T_{\mathrm{s}}^{3/2}$ in the case of helium, while gas velocity scales as $T_{\mathrm{s}}^{1/2}$ according to equation (1). Because the number of collisions results from r times the duration of the expansion Δt taken as inversely proportional to gas velocity, we finally have

$$\tilde{\beta} \propto T_{\mathrm{s}}^{1/\gamma-1} \Rightarrow \tilde{\beta} = \tilde{\beta}_0 \cdot \mathrm{e}^{-3t_{\mathrm{res}}/2\tau}. \tag{6}$$

The average collision effectiveness $\langle\alpha\rangle$ is assumed here as fixed for all the clusters under investigation and is included in the pre-factor $\tilde{\beta}_0$. The carrier gas stagnation temperature time constant τ is related to the gas release time constant τ_{r} (according to stagnation chamber volume and nozzle conductivity) by the relation $\tau = \tau_r \cdot \gamma/(\gamma - 1)$ whose value is determined as 110 ms from an independent direct measurement (a residence time-resolved partial ion yield measurement on molecular oxygen seeded in the supersonic He beam).

With ξ_0, ξ_1, ξ_2, $v_{\mathrm{gas},0}$ and $\tilde{\beta}_0$ as free parameters, the least-square fitting procedure shows an increasing trend for the D^*/D ratio with increasing residence time of Ti clusters (from ~ 0.8 to $\sim$0.9 in the range of 15–40 ms).

A numerical solution of the expression for $D^* - D$ given in [27] is consistent with the observed ξ values only if the observation scale r_{obs} is greater than $\sim$1.1 nm; this result holds for any decay rate of the cut-off function used in the description of density correlation. The value of the observation scale r_{obs} is determined from the normalized observation scale X of [27] as $r_{\mathrm{obs}} = X \cdot r_{\mathrm{cluster}}$ (iteration of the numerical solution is needed because cluster size r_{cluster}, determined from the observed m values, scales with the obtained fractal dimension). This should be interpreted as a lower limit to the inner scale of the fractal-like physical object imposed by finite primary particle size of the aggregates. Based on the comparison between the mass of a primary particle of this size, and the observed cluster mass, this solution would then imply a typical number of primary particles per cluster not greater than ~ 4, a situation that is not compatible with the observation of a fractal-like scaling of σ versus m. The experimental result must thus be interpreted assuming $D > 2$; this means that $D^* = 2$ and $D = 2/\xi$.

The observed increasing trend for ξ results therefore, as shown in figure 4, in a decreasing trend for the fractal dimension of the Ti clusters with increasing residence time (from $\sim$2.5 to $\sim$2.2 in the range of 15–40 ms). This result gives quantitative and unambiguous confirmation of a picture already suggested for the interpretation of the fragmentation pattern involved in the cluster–VUV photon interaction [19], which describes the nano-objects formed by the PMCS as super-aggregates of primary particles rather than compact spherical-shaped objects. This picture is also in agreement with previous observations of Alayan *et al* [6], who performed an extensive tunnel electron microscopy analysis on supported transition metal clusters grown in the gas phase under similar conditions (in a laser vaporization cluster source) and could identify a transition from compact to ramified particle structures at very small particle sizes.

The decrease of fractal dimension with decreasing stagnation temperature along with growing residence time (the stagnation temperature is related to the molecular beam velocity through equation (1)) agrees qualitatively with the common understanding of the coagulation process: due to lower atomic mobility and a lack of significant neck growth between colliding primary particles, coalescence slows down in the low temperature conditions resulting in soft agglomerates with a larger surface-to-volume ratio and excess surface energy [5] held together by van der Waals forces [3].

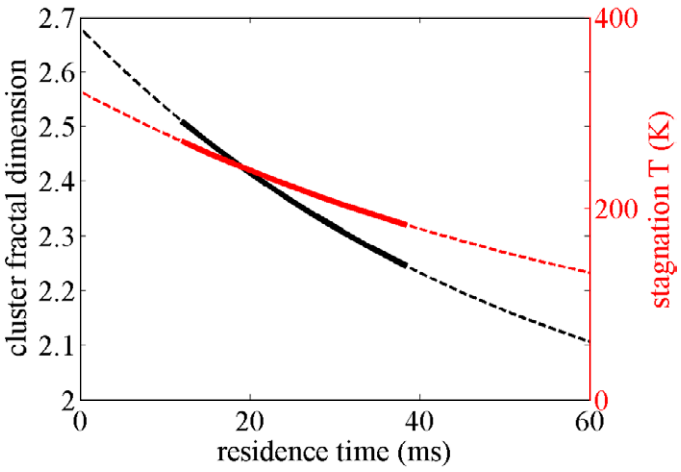

Figure 4. Residence time evolution of the cluster fractal dimension (black) and the carrier gas stagnation temperature (red) as determined by the least-square fitting procedure described in the text. The full lines represent the result in the investigated residence time, whereas dashed lines show extrapolation according to the assumed empirical model for gas evolution.

5. Conclusions

In summary, we have developed an approach for on-line tracking of gas-phase cluster morphology providing a feedback handle for tuning the working conditions of a nanoparticle source towards a specific desired agglomeration level. The size of primary particles and their density and temperature in the source are the most relevant variables for defining the transition from the coalescent regime to fractal aggregation [2, 34, 35]. We believe that this technique represents a unique tool for the characterization of the morphology of ultrafine gas-phase nanoparticles, providing access to real-time quantitative investigations of nanoscale objects in a molecular beam. The method can provide the necessary feedback for an improvement of the gas-phase particle formation and manipulation processes, as well as for the development of nanoparticle growth and transport models.

Appendix

In this appendix we provide the reader the details of calculations leading to expression (2), which puts in explicit form the established relationship between the velocity slip of clusters seeded in a supersonic expansion and their collisional cross section.

It is convenient to describe collisions in a reference frame moving with a velocity v_{gas} equal to the average carrier gas velocity and where the carrier gas is thus essentially at rest. In this frame, the velocity $\tilde{v}$ of a particle with mass m is changed by one central elastic collision with the carrier gas (mass m_{gas}) to the new value $\tilde{v}'$ with

$$\tilde{v}' = \tilde{v}\left(\frac{m - m_{\mathrm{gas}}}{m + m_{\mathrm{gas}}}\right). \tag{A.1}$$

This directly yields expression (A.2) for the particle velocity in the laboratory reference frame after k collisions, as provided by Wrenger and Meiwes-Broer [25]:

$$v_k\,(m) = v_{\text{gas}} \cdot \left[1 - \left(\frac{m - m_{\text{gas}}}{m + m_{\text{gas}}}\right)^k\right]. \tag{A.2}$$

For any kind of collision, in the reference frame travelling with the gas, we can write the conservation of momentum along the direction of carrier gas motion as

$$m\tilde{v} = m_{\text{gas}}\tilde{v}'_{\text{gas}} + m\tilde{v}'. \tag{A.3}$$

As our aim is to evaluate the average effect of multiple collisions, we can limit the discussion to the effects of collisions on the momentum projection along the carrier gas motion direction; as a matter of fact, under axial symmetry conditions, the mean momentum transfer along directions perpendicular to the axis is zero. We can then write in general $\tilde{v}'_{\text{gas}} = 2\alpha\tilde{v}$, where $\alpha_{\min} \leqslant \alpha < 1$ accounts for the actual momentum transfer occurring in the collision. The limit of maximum momentum transfer, corresponding to the case of centred elastic collisions with $m \gg m_{\text{gas}}$, is indeed accounted for by $\tilde{v}'_{\text{gas}} = 2\tilde{v}$, whereas $\alpha_{\min}$, which is zero in the case of hard-sphere collisions, can assume in the most general case also negative values taking into account e.g. the possible gas adsorption and desorption processes with diffuse emission over the whole solid angle [24]. Under this parameterization, momentum conservation means

$$\tilde{v}' = \tilde{v}\frac{m - 2\alpha m_{\text{gas}}}{m}, \tag{A.4}$$

which can be rewritten as

$$\tilde{v}'_N = \tilde{v}_N \left(\frac{m - m_{\text{gas}}}{m + m_{\text{gas}}}\right)^{\left[\log\left(\frac{m-2\alpha m_{\text{gas}}}{m}\right)/\log\left(\frac{m-m_{\text{gas}}}{m+m_{\text{gas}}}\right)\right]} \approx \tilde{v}\left(\frac{m - m_{\text{gas}}}{m + m_{\text{gas}}}\right)^{\alpha}, \tag{A.5}$$

where the approximation holds if $m_N \gg m_{\text{gas}}$.

After k collisions and in the laboratory reference frame, the average particle velocity is thus

$$\langle v_k\,(m)\rangle \approx v_{\text{gas}}\left[1 - \left(\frac{m - m_{\text{gas}}}{m + m_{\text{gas}}}\right)^{\langle\alpha\rangle k}\right]. \tag{A.6}$$

The general form of the particle velocity evolution after collision with the carrier gas molecules is thus the same, when $m_N \gg m_{\text{gas}}$, as that for the simple central elastic collision model after the total number of collisions is scaled by an effectiveness parameter $\langle\alpha\rangle$ with $0 < \langle\alpha\rangle < 1$. The actual value of $\langle\alpha\rangle$ depends on the nature of gas–particle interaction [36] and can in general be affected by particle morphology [26], taking into account the balance of diffuse versus elastic scattering [24]. Molecular dynamics and numerical integration may provide a useful means for the quantification of the $\langle\alpha\rangle$ values characteristic of different scattering processes.

For given expansion conditions the number of collisions can be assumed to scale with the geometric cross section σ of the particle (the projection of the particle geometry onto a plane perpendicular to the direction of carrier gas motion) [26], so the velocity of clusters of mass m, which undergo $k\langle\alpha\rangle = \beta \cdot \sigma$ effective collisions in the forward direction along the jet expansion, can be modelled by

$$v\,(m;\sigma) = v_{\text{gas}} \cdot \left[1 - \left(\frac{m - m_{\text{gas}}}{m + m_{\text{gas}}}\right)^{\beta\cdot\sigma}\right], \tag{A.7}$$

which corresponds to equation (2).

References

[1] de Heer W A 1993 *Rev. Mod. Phys.* **65** 611–76
[2] Lehtinen K E J, Windeler R S and Friedlander S K 1996 *J. Colloid Interface Sci* **182** 606–8
[3] Flagan R C and Lunden M M 1995 *Mater. Sci. Eng.* A **204** 113–24
[4] Xiong Y and Pratsinis S E 1993 *J. Aerosol Sci.* **24** 283–313
[5] Wu M K and Friedlander S K 1993 *J. Aerosol Sci* **24** 273–82
[6] Alayan R, Arnaud L, Broyer M, Cottancin E, Lermé J, Vialle J L and Pellarin M 2006 *Phys. Rev.* B **73** 125444
[7] Yang G and Biswas P 1999 *J. Colloid Interface Sci.* **211** 142–50
[8] Dekkers P J and Friedlander S K 2002 *J. Colloid Interface Sci.* **248** 295–305
[9] Kammler H K, Beaucage G, Kohls D J, Agashe N and Ilavsky J 2005 *J. Appl. Phys.* **97** 054309
[10] Schmidt-Ott A 1988 *J. Aerosol Sci.* **19** 553–63
[11] Tsyganov S, Kästner J, Rellinghaus B, Kauffeldt T, Westerhoff F and Wolf D 2007 *Phys. Rev.* B **75** 045421
[12] Wang G M and Sorensen C M 1999 *Phys. Rev.* E **60** 3036–44
[13] Virtanen A, Ristimäki J and Keskinen J 2004 *Aerosol Sci. Technol.* **38** 437–46
[14] Rockenberger J, Nolting F, Luening J, Hu J and Alivisatos A P 2002 *J. Chem. Phys.* **116** 6322
[15] Kanu A B, Dwivedi P, Tam M, Matz L and Hill H H Jr 2008 *J. Mass Spectrom* **43** 1–22
[16] Jarrold M F and Constant V A 1991 *Phys. Rev. Lett.* **67** 2994–97
[17] Hunter J M, Fye J L, Jarrold M F and Bower J E 1994 *Phys. Rev. Lett.* **73** 2063–66
[18] Barborini E, Piseri P and Milani P 1999 *J. Phys. D: Appl. Phys.* **32** L105
[19] Piseri P, Mazza T, Bongiorno G, Devetta M, Coreno M and Milani P 2008 *J. Electron Spectrosc. Relat. Phenom.* **166–167** 28–37
[20] Scoles G (ed) 1987 *Atomic and Molecular Beam Methods* vol 1(New York: Oxford University Press)
[21] DePaul S, Pullman D and Friedrich B 1993 *J. Phys. Chem.* **97** 2167–71
[22] Milani P and Iannotta S 1999 *Cluster Beam Synthesis of Nanostructured Materials* (Berlin: Springer)
[23] Broyer M, Cabaud B, Hoareau A, Melinon P, Rayane D and Tribollet B 1987 *Mol. Phys.* **62** 559–72
[24] Epstein P S 1924 *Phys Rev.* **23** 710
[25] Wrenger Bu and Meiwes-Broer K H 1997 *Rev. Sci. Instrum.* **68** 2027–30
[26] Meakin P, Donn B and Mulholland G W 1989 *Langmuir* **5** 510–18
[27] Nelson J A, Crookes R J and Simons S 1990 *J. Phys. D: Appl. Phys.* **23** 465–68
[28] Halpern A M and Glendening E D 1996 *J. Mol. Struct.* **365** 9–12
[29] Tafreshi H V, Piseri P, Benedek G and Milani P 2006 *J. Nanosci. Nanotechnol.* **6** 1140–49
[30] Blyth R R *et al* 1999 *J. Electron Spectrosc. Relat. Phenom.* **101–103** 959–64
[31] Mazza T 2007 Synchrotron light characterization of free metal and oxide nanoparticles *PhD Thesis* Università degli Studi di Milano
[32] Hoener M, Bostedt C, Schorb S, Thomas H, Foucar L, Jagutzki O, Schmidt-Böcking H, Dörner R and Möller T 2008 *Phys. Rev.* A **78** 021201
[33] Lubman D M, Rettner C T and Zare R N 1982 How isolated are molecules in a molecular beam? *J. Phys. Chem.* **86** 1129–35
[34] Zachariah M R and Carrier M J 1999 *J. Aerosol Sci.* **30** 1139
[35] Mitchell P and Frenklach M 2003 *Phys. Rev.* E **67** 061407
[36] Li Z and Wang H 2005 *Phys. Rev. Lett.* **95** 014502